

## SHORT COMMUNICATION

### A NOTE ON THE SOLUTION TO THE DIFFUSION EQUATION

YARLONG WANG\*

*Petro-Geotech Inc., 100 Discovery Place One, 3553-31 St. N.W., Calgary, Alberta, Canada T2L 2K7*

#### SUMMARY

Three methods (Gauss–Legendre method, Stehfest method and Laplace transform method) are used to evaluate a solution of a coupled heat–fluid linear diffusion equation. Comparing with the results by Jaeger, the accuracy and efficiency of the Stehfest and Gauss–Legendre methods and the limitations of the truncated solutions obtained by Laplace transformation are discussed. It is concluded that the Stehfest method gives accurate results and is numerically more efficient than the other two methods, particularly for the solutions in early time. Two transformations with  $u = -\ln(x)$  and  $u = \arctan(x\pi/2)$ , where  $u$  is the original integral variable, are considered in the Gauss–Legendre method.

KEY WORDS: heat–fluid–stress diffusion; Gauss–Legendre; Laplace transform; Stehfest method

#### INTRODUCTION

To describe a single phase fluid flow problem, a couple linear diffusion equation for a 2D circular wellbore in an isotropic, homogeneous low-permeability porous medium may be written as<sup>1</sup>

$$c\nabla^2 p = \partial p / \partial t - c_t \partial T / \partial t \quad (1)$$

where  $\nabla^2 = 1/r \partial/\partial r + \partial^2/\partial r^2$  and the definitions for the variables used may be found in Appendix II.

Furthermore, a conductive heat flow in such a medium may be described by the following linear diffusion equation:

$$c_0 \nabla^2 T = \partial T / \partial t \quad (2)$$

where  $c_0$  is the thermal diffusivity of the bulk medium. The solutions to the temperature change and pore pressure change fields for this borehole problem may be obtained by solving the coupled equations (1) and (2).

Carslaw and Jaeger<sup>2</sup> presented various solutions for the heat conduction problem; corresponding to different boundary conditions these solutions may also be used to analyse the pore fluid pressure diffusion processes [equation (2)]. However, some of these closed-form solutions involve integrals which are not tractable and evaluating these integrals numerically complicates solution application. Thus, this paper will focus on seeking efficient solutions to these integrals.

---

\* Previously at: Shell Canada Ltd., P.O. Box 2506, Calgary, Alberta, Canada T2P 3S6

Although Jaeger<sup>3</sup> presented a comprehensive analysis of a heat diffusion problem only with a Type I boundary condition, and McTigue<sup>1</sup> studied the coupled heat-fluid diffusion problem for the Type II boundary condition, the numerical solution procedure has not been fully addressed. Neither Jaeger nor McTigue presented an analysis of the methods they used, nor rigorously described the numerical procedures. For practical interests in petroleum and hydrogeological engineering, it is important to document the efficiency of the methods and the possible error involved. The Gauss-Legendre method is conveniently employed to evaluate the half infinite integral in the general solution. A variable transformation is required that transforms the semi-infinite domain into a finite domain. It will be shown in this note that no efficient or even unstable solution may be obtained of this diffusion equation if the semi-infinite domain is transformed into a finite one inappropriately.

To address both the accuracy and the computational efficiency of the Gauss-Legendre method to such a solution type, a proven, accurate method by Stehfest,<sup>4</sup> which is also validated by comparing with the result by Jaeger,<sup>3</sup> is used. Only the Type I boundary condition will be considered. Talbot<sup>5</sup> presented an alternative inverse transforming algorithm which has also been applied in practice<sup>6-8</sup> and only the Stehfest method will be used. The possible numerical error, corresponding numerical difficulty, and limitation of the truncated solution are also evaluated.

### BOUNDARY CONDITIONS AND THE CLOSED-FORM SOLUTIONS

In practice, to evaluate the hydraulic conductivity of the rock formation, a boundary condition of constant wellbore pressure and temperature changes may be imposed when leak-off and constant head tests are conducted.<sup>9</sup> For coupled thermal problems, one can solve equation (2) first. The Type I boundary conditions are

$$T(r, 0) = 0; \quad T(a, t) = T_w - T_0; \quad T(\infty, t) = 0 \quad (3)$$

where  $T_0$  is the initial temperature and  $T_w$  is an imposed wellbore temperature. A general procedure for solving this problem is to transform equation (2) into the Laplace domain.<sup>2</sup> The corresponding complete solution obtained for the initial condition and Type I boundary conditions given in (3) is

$$s\bar{T}/(T_w - T_0) = K_0(\xi_1)/K_0(\beta_1) \quad (4)$$

where the overbar denotes Laplace transformation,  $K_0$  is the modified Bessel function of the second kind of order zero,  $s$  is the Laplace parameter and  $\xi_1 = r\sqrt{(s/c_0)}$ ,  $\beta_1 = a\sqrt{(s/c_0)}$ . Equation (4) will be used in conjunction with the Stehfest method.

The general solution for equation (4) can be written as:<sup>2</sup>

$$T/(T_w - T_0) = 1 + \frac{2}{\pi} \int_0^\infty \exp(-u^2 c_0 t) \frac{I du}{u} \quad (5)$$

$$I = \frac{J_0(ur) Y_0(ua) - J_0(ua) Y_0(ur)}{Y_0^2(ua) + J_0^2(ua)}$$

Equation (5) is the general solution for heat diffusion near a wellbore subjected to Type I boundary condition. It must be solved numerically and all symbols will be defined later in Appendix II. A truncated solution near a borehole and early time conditions may be obtained following Rice and Cleary:<sup>10</sup>

$$T/(T_w - T_0) \approx \sqrt{\left(\frac{a}{r}\right)} X \quad (6)$$

This is a simplified expression for small time solution which was derived by Carslaw and Jaeger<sup>2</sup> first, i.e.

$$T/(T_w - T_0) \approx \left[ \sqrt{\left(\frac{a}{r}\right)} - \frac{(a-r)^2}{8ar^{3/2}} + \frac{(9a^2 - 2ra - 7r^2)}{128a^{3/2}r^{5/2}} [1 + X^2] \right] X \\ + \frac{a-r}{4} \exp(-X^2) \left[ \sqrt{\left(\frac{c_0 t}{ar^2 \pi}\right)} - \frac{(9a^2 - 2ra - 7r^2)}{32r^{5/2}a^{3/2}\sqrt{(c_0 t \pi)}} \right] \quad (7)$$

where

$$X = \operatorname{erf} c[(r-a)/2\sqrt{(c_0 t)}]$$

The above truncated solutions are only approximations of the general solution in (5). To assess the limitations of these solutions, exact solutions are required. Compared with the limited exact result provided by Jaeger,<sup>3</sup> the Stehfest method<sup>4</sup> gives both accurate and stable solutions. This method thus is used to provide the reference results. Through this comparison, the applicable range of the truncated solutions may be defined.

To obtain a complete solution to the coupled heat-fluid problem, however, equation (1) subject to (3) must also be solved. The boundary condition for pore pressure change may be written as

$$p(r, 0) = 0, \quad p(a, t) = p_w - p_0, \quad p(\infty, t) = 0 \quad (8)$$

The solution to equation (1) subject to the initial and boundary conditions (8) may be written as<sup>11</sup>

$$\frac{s\bar{p}}{(p_w - p_0)} = \frac{K_0(\xi)}{K_0(\beta)} - \frac{c_t}{(1 - c/c_0)} \frac{(T_w - T_0)}{(P_w - P_0)} \left[ \frac{K_0(\xi)}{K_0(\beta)} - \frac{K_0(\xi_1)}{K_0(\beta_1)} \right] \quad (9)$$

and an inversion transformation leads to

$$p = \left( p_w - p_0 - \frac{c_t(T_w - T_0)}{1 - c/c_0} \left[ 1 + \frac{2}{\pi} \int_0^\infty e^{-cu^2 t} \frac{I du}{u} \right] + \frac{c_t(T_w - T_0)}{1 - c/c_0} \left[ 1 + \frac{2}{\pi} \int_0^\infty e^{-c_0 u^2 t} I \frac{du}{dt} \right] \right) \quad (10)$$

where  $\xi = r\sqrt{(s/c)}$  and  $\beta = a\sqrt{(s/c)}$ . Note that even though Wang and Papamichos<sup>11</sup> obtained the above solution, only a truncated result was analysed. A discussion to the complete solution evaluation therefore is presented in this note.

The two integrals in equation (10) have an identical form to that in (5). Hence, the numerical procedure, which adequately solves the temperature change equation, is also applicable for the analysis of the pore pressure. In the following, therefore, only the solution to the temperature equation subjected to (3) will be discussed.

## NUMERICAL PROCEDURES

### *The Gauss-Legendre method*

A routine to generate Gaussian points is used so that we may estimate the effect of the Gaussian point number on the numerical accuracy; this routine also provides the corresponding weighting function.<sup>12</sup> Now, the evaluation of the integral may proceed.

In order to evaluate the infinite integral in equation (5), the Gauss-Legendre method is used. At first, the  $0-\infty$  domain is divided into  $0-\varepsilon$  and  $\varepsilon-\infty$ . Thus the singularity point for the lower limit for the semi-infinite integration is removable, provided the integral for  $0-\varepsilon$  is treated. The detailed treatment can be found in Appendix I. Secondly, a simple variable transformation is conducted by introducing a new variable  $x$  so that the variable of integration in (5) or in  $W_2$  of (13) becomes  $u = -\ln x$ . Many textbooks<sup>10</sup> suggest the use of this transformation, which transforms the semi-infinite domain into a finite between 0 and 1. However, such a transformation can create numerical problems for early time solutions as shown later. Alternatively, another transformation, in which  $u = \arctan(x\pi/2)$ , also transforms the semi-infinite domain into a finite one (0-1).

### *The Stehfest method*

To offer an alternative approach to the Gauss-Legendre method and to minimize computational effort, an approximate Laplace inversion method is used.<sup>4,13</sup> Rather than dealing with the integral from equation (5), this approximate method is based on equation (6). The Stehfest method has been extensively used, especially in petroleum engineering, due to its accuracy, efficiency and stability. This method is based on sampling inversion data according to a delta series. The approximate solution in time is given by the following formula,

$$f(t) = \frac{\ln 2}{t} \left[ \sum_{n=1}^N C_n \bar{f}\left(n \frac{\ln 2}{t}\right) \right] \quad (11)$$

where the coefficient  $C_n$  is defined by

$$C_n = (-1)^{n+N/2} \sum_{k=(n+1)/2}^{\min(n, N/2)} \frac{k^{N/2} (2k)!}{(N/2 - k)! k! (k-1)! (n-k)! (2k-n)!} \quad (12)$$

The number of terms ( $N$ ) in the series is even and is typically in the range of 10-20.

## RESULTS AND DISCUSSION

### *Results by the truncated solutions*

The applicability of the truncated solution (7) has been comprehensively documented.<sup>3</sup> Jaeger<sup>3</sup> suggested that the truncated solution may be applicable when  $tc_0/a^2 < 0.1$ . The calculations made for this paper indicate that the truncated solution (6), which is the first truncated term in the solution (7) may give a better approximation to the exact solution for  $tc_0/a^2 > 1$  than when (7) is used (Figure 1).

### *Results by the Gauss-Legendre method*

Because a well-behaved integrand can be essential to achieve the stable and accurate numerical solution for the integral in (5) the behaviour of the integrand after the first transformation where  $u = -\ln(x)$  is analyzed and presented in Figure 2. The two boundary points (i.e.  $x = 0$  and 1) signify important aspects of the numerical trend. Sharp 'gradients' exist near both  $x = 0$  and 1, which may cause numerical error. Figure 3 shows the numerical results, and the effect of the number of Gauss points chosen for the solution. It can be observed that no stable solution can be produced using this transformation for the early time, even though up to 2500 Gaussian points have been used. The oscillations in the early time results may be caused by this specific

transformation for numerical integration, as two underlined external boundaries are created (Figure 2).

To cope with this numerical oscillation problem, transformation 2, where  $u = \arctan(x\pi/2)$ , is also employed. The behaviour of the corresponding integrand is presented in Figure 4. While

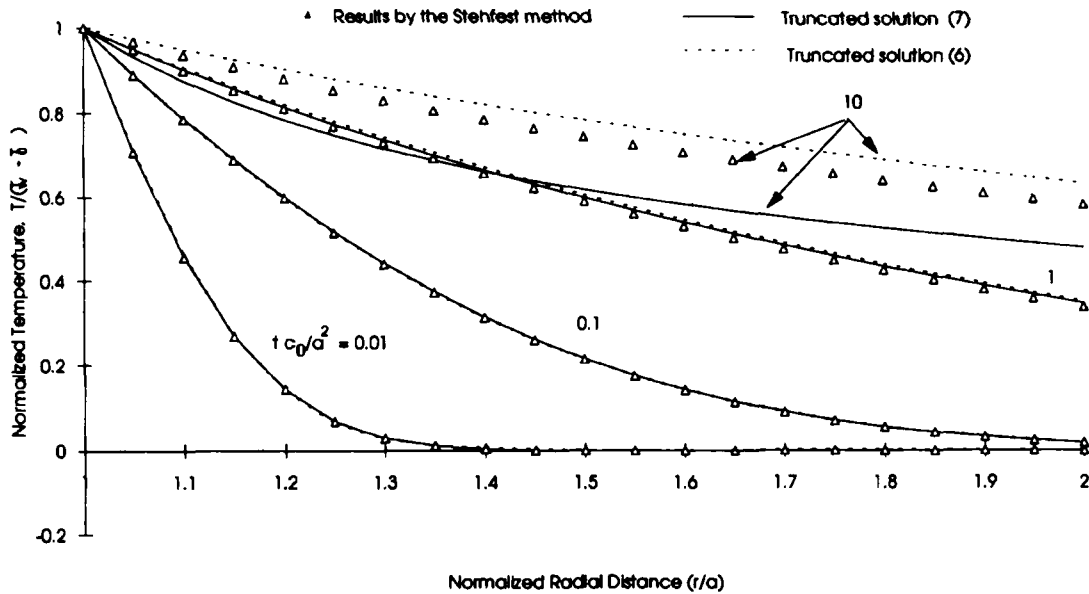


Fig. 1. Comparison between the numerical and the truncated solutions. It may be observed that the truncated solutions and the numerical solutions are similar for  $t c_0 / a^2 > 0.01$

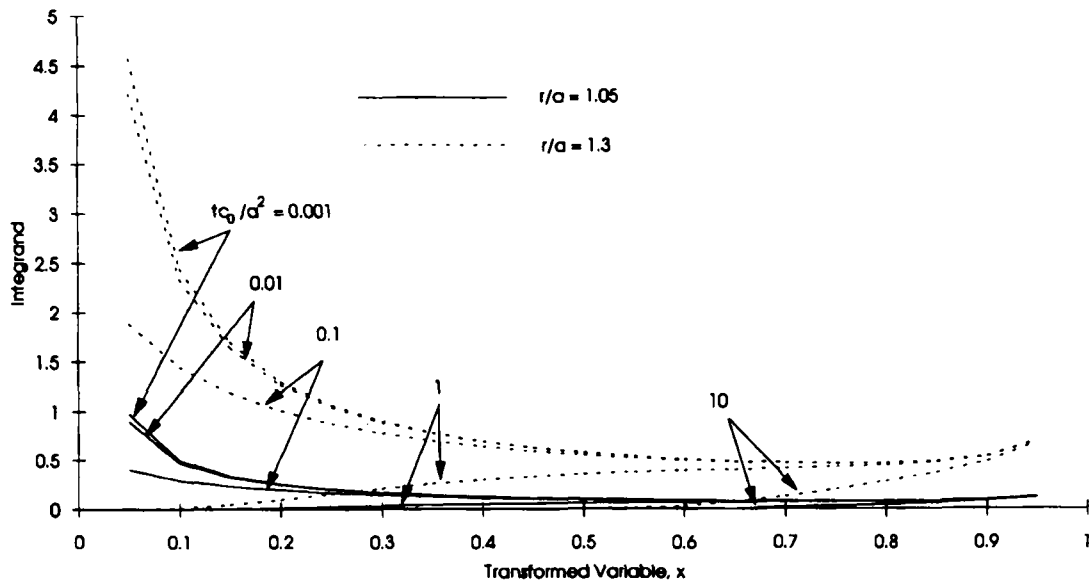


Fig. 2. Behaviour of the integrand of equation (5) in the spatial and time spaces ( $u = \ln(x)$ ). There are two singularities existing at  $x = 0$  and  $x = 1$  ( $x$  here is the transformed variable). Near these two boundaries unstable numerical results may be induced.

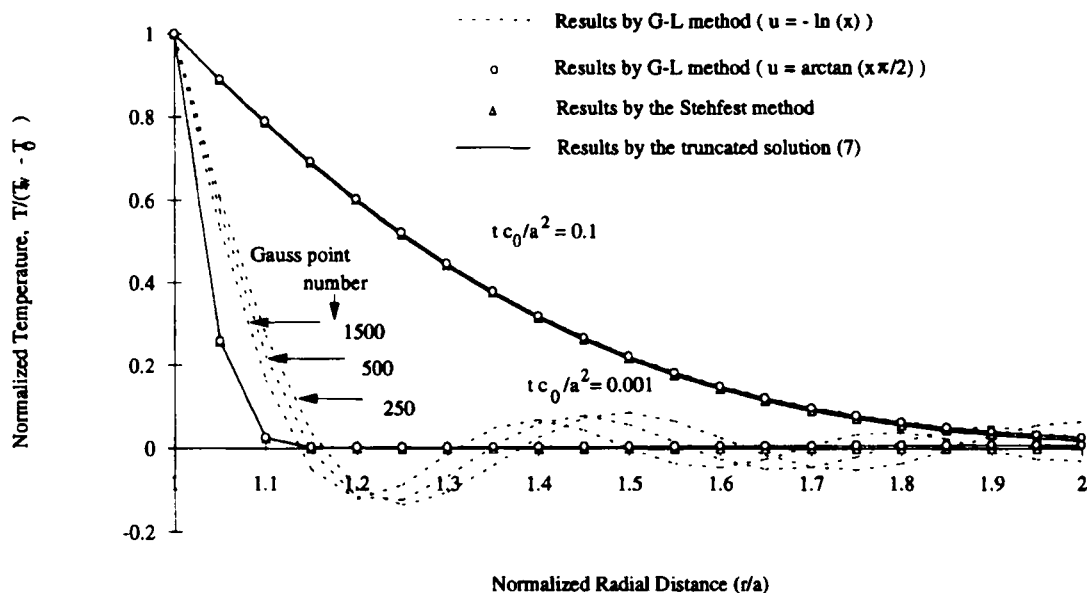


Fig. 3. Comparisons between the Gauss-Legendre method, the Stehfest numerical inversion approximation, and the truncated solution, equation (7). It may be shown that the early time solution by transformation 1 of the Gauss-Legendre method is unstable, while an appropriate transformation may give a stable solution

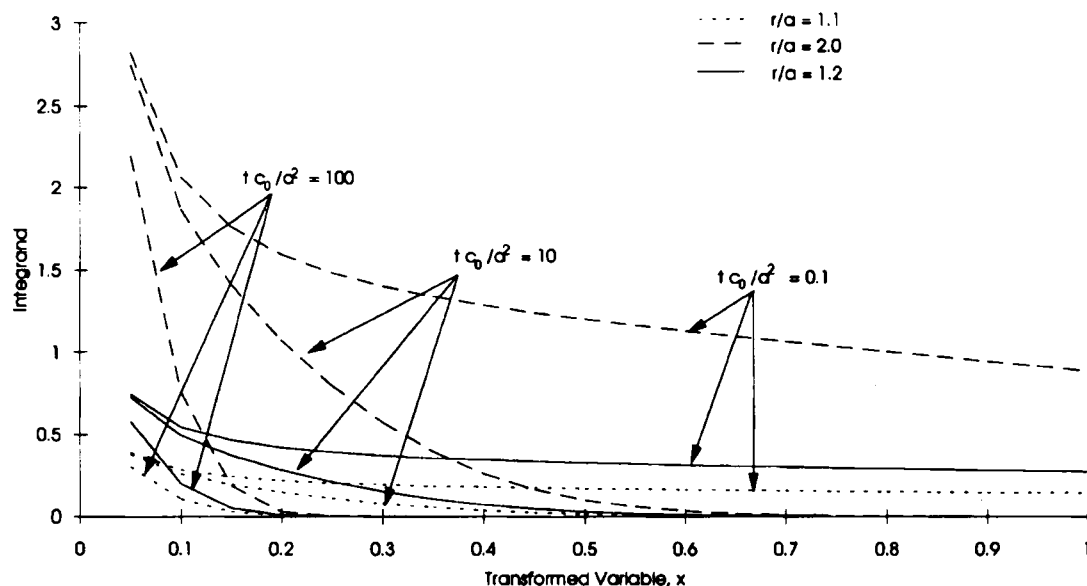


Fig. 4. Behaviour of the integrand in the spatial and time spaces ( $u = \arctan(x\pi/2)$ ). It may be observed that a singularity point only exists at  $x = 0$ , while the behaviour at  $x = 1$  is smooth, in contrast to that by transformation 1. This curve implies that numerical instability for the problem considered may be removable once the internal singularity is treated

abnormal behaviour exists at the internal boundary, the integrand curve is smooth at the external boundary. Because the singularity at the internal boundary has been removed, the fact that the former result is unstable but the latter is stable indicates that the untreated singularity at the external boundary for transformation 1 provokes unstable numerical solution for the early time. Specifically, a reasonably accurate result can be obtained by transformation 2 if more than 200 Gauss points are used. In the particular example plotted in Figure 3, 800 Gauss points are used for the solution by both transformations, except for an early time solution, in which more than 1500 Gauss points have been used for that by transformation 1 for the early time.

For numerical accuracy, the singular point near  $u = 0$  must be removed as shown in Appendix I. Figure 5 shows the effect of the singular point near the lower limit. An additional 10 per cent error may be caused if this singular point is not treated appropriately. McTigue<sup>2</sup> also conducted such an approximate solution by removing the singular point; he used  $10^{-7}$  as the initial integration point in a half-positive space.

### Results by the Stehfest method

Figure 3 also presents the results of the Stehfest method. This method gives accurate and stable results particularly at early time. The computational time required for this method is also much less than those by the Gauss–Legendre method used. For example, to produce the same results as shown in Figure 3, a PC 486 computer requires about 30 min for the Gauss–Legendre method under transformation 1 (1500 Gauss points are used), compared to less than 1 s for the Stehfest method. Another advantage of using the Stehfest method is that the singular point, which complicates the Gauss–Legendre method, simply does not exist. By this method, the tedious algebraic deviations, which in many cases can be extremely difficult or impossible, may be avoided. Table I provides the numerical results of the three different methods.

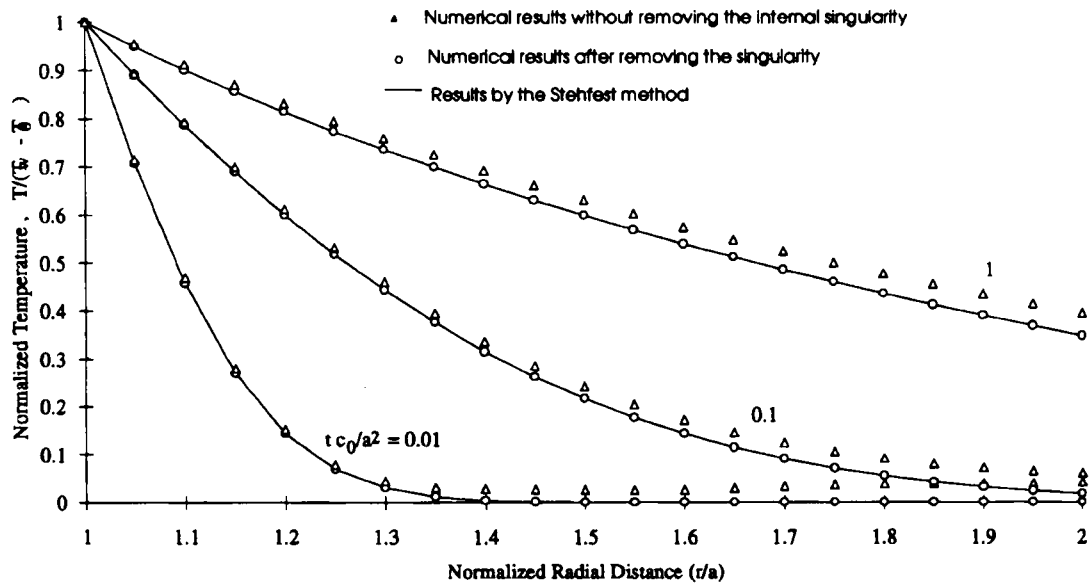


Fig. 5. The result by the Gauss–Legendre method without the treatment of the singularity at the lower limit.

Table I. Exact results by Jaeger, two truncated solutions, numerical results by the Gauss-Legendre method with two different transformations, and those by the Stehfest method. Truncated solution 1 denotes the expanded truncated solution [i.e. from equation (8)]. Truncated solution 2 contains the further truncated solution [i.e. from equation (7)]. Transformation 1 denotes the case where  $u = \arctan(x\pi/2)$ , and transformation 2 represents the case in which  $u = -\ln(x)$ . For both Gauss-Legendre solutions 800 Gauss points are used. Here  $t^* = c_0 t/a^2$

$r/a$	Exact result	Stehfest solution	Truncated solution 1	Truncated solution 2	GL result with transformation 1	GL result with transformation 2
$t^* = 0.001$						
0.1	1.0	1.0	1.0	1.0	1.0	1.0
1.2	0.0	0.0	0.0	0.0	0.1120	0.0022
1.4					0.5250	0.0040
1.6					-0.0120	0.0056
1.8					-0.0020	0.0070
2.0					0.0340	0.0083
$t^* = 0.01$						
1.0	1.0	1.0	1.0	1.0	1.0	1.0
1.2	0.144	0.1437	0.1438	0.1436	0.1427	0.1460
1.4	0.004	0.0039	0.0040	0.0040	0.0010	0.0080
1.6	0.0	0.0	0.0	0.0	0.0035	0.0056
1.8					0.0035	0.0070
2.0					0.0120	0.0083
$t^* = 0.1$						
1.0	1.0	1.0	1.0	1.0	1.0	1.0
1.2	0.601	0.6007	0.6005	0.5977	0.6024	0.6029
1.4	0.316	0.3159	0.3159	0.3136	0.3192	0.3200
1.6	0.143	0.1432	0.1423	0.1421	0.1477	0.1489
1.8	0.055	0.0555	0.0554	0.0549	0.0609	0.0624
2.0	0.018	0.0182	0.0181	0.0179	0.0246	0.0264
$t^* = 1.0$						
1.0	1.0	1.0	1.0	1.0	1.0	1.0
1.2	0.821	0.8202	0.8144	0.8102	0.8227	0.8232
1.4	0.672	0.6715	0.6645	0.6569	0.6749	0.6757
1.6	0.546	0.5459	0.5399	0.5308	0.5505	0.5517
1.8	0.440	0.4401	0.4354	0.4261	0.4458	0.4473
2.0	0.351	0.3513	0.3478	0.3391	0.3597	0.3579
$t^* = 10$						
1.0	1.0	1.0	1.0	1.0	1.0	1.0
1.2	0.903	0.9027	0.7840	0.8803	0.9044	0.9049
1.4	0.820	0.8205	0.6618	0.7849	0.8236	0.8245
1.6	0.749	0.7494	0.5825	0.7062	0.7538	0.7550
1.8	0.687	0.6869	0.5251	0.6395	0.6925	0.6940
2.0	0.631	0.6313	0.4802	0.5820	0.6378	0.6396

The Stehfest method is also recommended for the solution on contaminant transport processes along a single fracture. Tang *et al.*<sup>14</sup> and Sudicky and Frind<sup>15</sup> presented solutions for solute transport in a single and multi-fracture network. Both single and double infinite integrals are involved. A special solution scan procedure has to be conducted, since the majority of the numerically significant portion extends in certain regions only. Even though the computational time required in their study is not significant, as no early time solute concentration is considered



and only 60–104 Gauss points are needed, the effort to achieve their solution, i.e. the lengthy derivation and scan processes, may be reduced if the Stehfest method is used. In contrast, Rowe and Booker's<sup>6–8</sup> use of the Talbot method for solute transport simulation in a 3D fracture network represents an alternative to direct evaluation of the solution.

### CONCLUSION

In conclusion, it is advisable to use the closed-formed solution [i.e. (6) or (7)] for  $tc_0/a^2 < 0.1$ . The Stehfest method may be used for the remainder of the time period, and the Gauss–Legendre method may only be employed if an appropriate transformation is used. In some cases, a combination of different transformations may be used for different periods of time so that stable and accurate results may be achieved. It is also interesting to note that for a later time approximation (e.g.  $tc_0/a^2 > 1$ ), the truncated solution (6), rather than solution (7), may be used. This gives a closer approximation to the exact solution even though (6) is a more simplified expression (5) than solution (7).

### APPENDIX I

The integrand in equation (5) is singular at the lower limit of integration,  $u = 0$ , and is thus difficult to evaluate numerically. In order to avoid this difficulty, the integral may be partitioned as

$$W = W_1 + W_2 = \frac{2}{\pi} \int_0^\varepsilon e^{-c_0 u^2 t} \frac{I du}{u} + \frac{2}{\pi} \int_\varepsilon^\infty e^{-c_0 u^2 t} \frac{I du}{u} \quad (13)$$

where  $\varepsilon$  is chosen as a small value. The second part on the right-hand side of the above equation may be evaluated numerically; however, the first part requires further approximation. For small  $\varepsilon$ , the integrand in the first term on the right-hand side of the above equation may be approximated as

$$W_1 \approx \frac{2}{\pi} \int_0^\varepsilon e^{-u^2 c_0 t} I \ln \frac{r}{a} \frac{1}{1 + (4/\pi^2) \ln(ua/2) + \gamma)^2} \frac{du}{u} \quad (14)$$

Furthermore, this may be integrated as

$$W_1 = \ln(r/a) \arctan(2/\pi [\ln(\varepsilon a/2) + \gamma]) + \pi/2 \ln(r/a) \quad (15)$$

where the Euler's constant  $\gamma = 0.5772$ . Substituting (15) into (13), the solution for the diffusion equation with a Type I boundary condition may be obtained.

### APPENDIX II

#### Notation

$a$	wellbore radius (m)
$r$	radial variable (m)
$c, c_0$	hydraulic and thermal diffusivity, respectively ( $\text{m}^2/\text{s}$ )

$c_t$	heat-fluid coupling coefficient (MPa/°C)
$C_n$	a coefficient for the Stehfest's method
$J_0, Y_0$	first and second kind of Bessel's functions of zero order, respectively
$K_0, K_1$	modified Bessel functions of the second kind of first and zero order, respectively
$p$	pore pressure variable (MPa)
$P_w, P_0$	wellbore and initial pore pressures, respectively (MPa)
$T$	temperature variable (°C)
$T_w, T_0$	wellbore and initial pore pressures, respectively (°C)
$t$	time variable (s)
$u, x$	original and transformed variables, respectively
$\xi_1, \beta_1$	$= r\sqrt{(s/c_0)}; a\sqrt{(s/c_0)}$ .

### ACKNOWLEDGEMENTS

This work was initially conducted in the University of Alberta. The author would like to express his gratitude to J. D. Scott of the University of Alberta for his financial support. The author would also like to thank C. van Kruijsdijk of Shell Canada, who has generously provided a numerical code for the Stehfest method. Finally, the discussion with E. Papamichos of IKU, Norway, as well as the critical review and useful suggestions by Dr. Y. Du of Stanford University and Miss M.D. Dumont of the University of Calgary are also deeply appreciated.

### REFERENCES

1. D. F. McTigue, 'Flow to a heated borehole in porous, thermoelastic rock: analysis', *Water Resource Res.*, **26**, 1763-1774 (1990).
2. H. S. Carslaw and J. C. Jaeger, *Conduction of Heat in Solids*. 2nd edn, Oxford University Press, New York, 1959.
3. J. C. Jaeger, 'Numerical values for the temperature in radial heat flow', *J. Math. Phys.*, **34**, 316-321 (1956).
4. H. Stehfest, 'Numerical inversion of Laplace transforms', *Commun. ACM*, **13**, 624 (1970).
5. A. Talbot, 'The accurate numerical integration of Laplace transforms', *J. Inst. Math. Appl.*, **23**, 97-120 (1979).
6. R. K. Rowe and J. R. Booker, 'Modelling of contaminant movement through fractured or jointed media with parallel fractures', *Proc. 6th Int. Conf. Numer. Methods Geomech.*, Innsbruck, 1988, pp. 855-862.
7. R. K. Rowe and J. R. Booker, 'A semi-analytic model for contaminant migration in a regular two and three dimensional fracture network: conservative contaminants', *Int. J. Numer. Methods Geomech.*, **13**, 531-550 (1989).
8. R. K. Rowe and J. R. Booker, 'A semi-analytic model for contaminant migration in a regular two and three dimensional fracture network: reactive contaminants', *Int. J. Numer. Methods Geomech.*, **14**, 401-425 (1990).
9. R. A. Freeze and J. A. Cherry, *Groundwater*, Prentice-Hall, Englewood Cliffs, NJ, 1979.
10. J. R. Rice and M. P. Cleary, 'Some basic stress diffusion solutions for fluid-saturated elastic porous media with compressible constituents', *Rev. Geophys.*, **14**, 227-241 (1976).
11. Y. Wang and E. Papamichos, 'An analytical solution for conductive heat flow and the thermally induced fluid flow around a wellbore in a poroelastic medium', *Water Resource Res.*, **36**, 3375-3384 (1994).
12. W. H. Press, S. A. Teukolsky, W. T. Vetterling and B. P. Flannery, *Numerical Recipes*, 2nd edn, Cambridge University Press, Cambridge 1992.
13. R. Piessens, 'Bibliography on numerical inversion of the Laplace transform and applications', *J. Comp. Appl. Math.*, **1**, 115-126 (1975).
14. D. J. Tang, E. O. Frind and E. A. Sudicky, 'Contaminant transport in fractured porous media: analytical solution for a single fracture', *Water Resource Res.*, **17**, 555-564 (1981).
15. E. A. Sudicky and E. O. Frind, 'Contaminant transport in fractured porous media: analytical solution for a single fracture', *Water Resource Res.*, **18**, 1634-1642 (1982).